JCTC Journal of Chemical Theory and Computation

Article

pubs.acs.org/JCTC

Exploring Potential Energy Surfaces of Electronic Excited States in Solution with the EOM-CCSD-PCM Method

Marco Caricato*

Gaussian, Inc., 340 Quinnipiac St., Bldg. 40, Wallingford, Connecticut 06492, United States

Supporting Information

ABSTRACT: The effect of the solvent on the structure of a molecule in an electronic excited state cannot be neglected. However, the computational cost of including explicit solvent molecules around the solute becomes rather onerous when an accurate method such as the equation of motion coupled cluster singles and doubles (EOM-CCSD) is employed. Solvation continuum models like the polarizable continuum model (PCM) provide an efficient alternative to explicit models, since the solvent conformational average is implicit and the solute−solvent mutual polarization is naturally accounted for. In this work, the coupling of EOM-CCSD and PCM in a state specific approach is presented for the evaluation of energy and analytic energy gradients. Also, various approximations are explored to maintain the computational cost comparable to gas phase EOM-CCSD. Numerical examples are used to test the different schemes.

1. INTRODUCTION

The efficient exploration of potential energy surfaces (PESs) of molecules in their electronic ground state is a fundamental success of computational chemistry[1−3] since it allows the investigation of chemical reactivity. The advent of methods able to describe electronic excited states has opened the door to studying all those processes that involve higher electronic states, from absorption and emission spectra to photochemical reactivity. In particular, accurate methods such as the equation of motion coupled cluster singles and doubles (EOM-CCSD)[4−9] are necessary to provide a reliable description of electronic excited states of isolated molecules. However, most chemistry happens in the condensed phase where the solvent significantly affects the properties of the solute. Therefore, a modeling of the solvent effect, even at a lower level of theory than the solute, is very important for realistic simulations.

Several approaches are available to introduce the solvent effect in high-level correlation methods.[10−20] Among these, continuum models such as the polarizable continuum model (PCM)[21,22] are particularly appealing when no direct solute−solvent interaction occurs (e.g., strong hydrogen bonds) since the conformational average of the solvent molecules around the solute is intrinsic in the model, and the solute−solvent mutual polarization is naturally included. PCM describes the solvent as a polarizable dielectric that contains the solute in a cavity of molecular shape built from interlocking spheres centered on the solute nuclei. The solvent response (solvent reaction field) to the presence of the solute electronic and nuclear density is expressed as an apparent charge spread on the cavity surface. A solvent interaction term is introduced in the molecular Hamiltonian, and the Schrödinger equation is solved iteratively until mutual polarization between the solute charge density and the solvent response is achieved.

The combination of continuum solvation models and CC methods was initially proposed by Christiansen and Mikkelsen.[23,24] More recently, Cammi extended it to the coupling of CCSD and PCM[25] with the perturbation theory energy and density (PTED) approach,[26,27] and Caricato et al. implemented and tested this approach.[28] However, since the PCM interaction term depends on the electronic density, its coupling with CC methods makes the calculation considerably more expensive than without PCM. This is because the calculation of the energy with CC methods only requires the solution of one set of nonlinear equations to compute the CC T amplitudes,[9,29] while the evaluation of the density requires the solution of another set of equations to compute the Λ amplitudes.[30,31] In comparison, self-consistent field methods like Hartree−Fock (HF) and density functional theory (DFT) do not show the same increase in computational cost since the electronic density and the energy are computed simultaneously. Therefore, I developed a series of methods to introduce an approximate PCM contribution in the CCSD wave function that recovers most of the solvent effect while maintaining the computational cost comparable to gas phase CCSD.[32,33]

The extension of PCM to excited states can be done within a linear response (LR) or state specific (SS) formalism.[22,34,35] Although the two approaches provide the same results for gas phase methods, they differ in solution. The origin of the difference is in the definition of the solvent response: in the LR approach, the solvent feels the solute transition density, while in the SS approach, the solvent feels the solute excited state density. It was shown that the latter approach is more physically meaningful,[35] and methods were proposed to correct the LR approach.[36] Christiansen and co-workers[24,37,38] used the LR approach to compute excited state energy and properties with CC methods and their solvation continuum model. Cammi developed a combination of EOM-CCSD and PCM in a SS approach,[39] and of symmetry-adapted cluster-configuration interaction (SAC−CI) and PCM in collaboration with Nakatsuji and co-workers.[40,41]

Special Issue: Berny Schlegel Festschrift

Received: May 14, 2012
Published: June 27, 2012

In this work, I present the theory for the coupling of EOM-CCSD and PCM with a SS Lagrangian formalism according to the PTED approach. The method introduced here is more general than that in ref 39, which is included as an approximation. Additionally, other approximate schemes are introduced that represent the EOM extension of the ground state CCSD-PCM methods in ref 32. All of the methods are implemented for the calculation of the energy as well as analytic energy gradients. However, in this paper, the PCM contribution is only limited to the equilibrium solvation regime.[22] This assumes that the time scale of the solvent response is similar to that of changes in the solute charge density. This assumption is valid for exploring the PES, whereas it is not for vertical transition processes. In the latter case, a nonequilibrium solvation regime should be invoked, where the solvent molecules and nuclei remain fixed while only the solvent electrons are considered fast enough to respond to the sudden change in the solute electronic density. Such a situation can be efficiently modeled with PCM[22] and will be considered in a future development of the methods proposed here.

The paper is organized as follows. The theory and implementation of the methods is presented in section 2. Numerical applications on test systems are described in section 3, while a discussion of the results and concluding remarks are presented in section 4.

2. THEORY

In this section, I present the theory for the combination of EOM-CCSD with PCM in a state specific approach. A Lagrangian formulation is used since it employs a more compact formalism. A review of the theory and implementation of the family of polarizable continuum models of solvation can be found in the literature[21,22,42−48] and will not be repeated here. In the following, the expression "*gas phase*" is loosely used to indicate the absence of PCM.

2.1. *Gas Phase* EOM-CCSD. Although the Lagrangian formulation of EOM-CCSD for the *gas phase* is well-known,[7] it is instructive to summarize it here to provide a parallelism with that in solution, especially when working approximations are introduced in the latter.

The EOM-CCSD Lagrangian for an excited state K can be formulated in two equivalent ways:

$$\mathcal{L}_K = \langle \Phi^0 | L_K [e^{-T} H e^T, R_K] | \Phi^0 \rangle + \langle \Phi^0 | (1 + \Lambda_K) e^{-T} H e^T | \Phi^0 \rangle + \omega_K (1 - \langle \Phi^0 | L_K R_K | \Phi^0 \rangle) \quad (1)$$

and

$$\mathcal{L}'_K = \langle \Phi^0 | L_K e^{-T} H e^T R_K | \Phi^0 \rangle + \langle \Phi^0 | \Lambda'_K e^{-T} H e^T | \Phi^0 \rangle + E_K (1 - \langle \Phi^0 | L_K R_K | \Phi^0 \rangle) \quad (2)$$

In eqs 1 and 2, Φ^0 is a reference determinant, usually the HF wave function. T is the CC excitation operator:

$$T = \sum_n t_n \tau_n \quad (3)$$

where n runs over the excitation manifold (single and double excitations for CCSD), τ_n is an excitation operator, and t_n is the corresponding amplitude. R_K and L_K are the right and left eigenvectors, respectively, of the non-Hermitian similarity-transformed Hamiltonian, $e^{-T} H e^T$:

$$R_K = r_0^K + \sum_n r_n^K \tau_n \quad (4)$$

$$L_K = l_0^K + \sum_n l_n^K \tau_n^\dagger \quad (5)$$

where $\tau_n^\dagger$ is a de-excitation operator. Λ_K and Λ'_K are also linear combinations of de-excitation operators, necessary when analytic gradients of the Lagrangian with respect to external perturbations are computed:[5−7]

$$\Lambda_K = \sum_n \lambda_n^K \tau_n^\dagger \quad (6)$$

$$\Lambda'_K = \sum_n \lambda_n'^K \tau_n^\dagger \quad (7)$$

The Lagrangian multipliers E_K and ω_K can be identified with the total energy of the Kth state and the transition energy from the CC ground state, respectively:

$$\omega_K = E_K - E_0 \quad (8)$$

where

$$E_0 = \langle \Phi^0 | e^{-T} H e^T | \Phi^0 \rangle \quad (9)$$

is the CC ground state energy. Intermediate normalization is used.

Equations for the t_n amplitudes can be obtained by imposing that the $\mathcal{L}_K$ (or $\mathcal{L}'_K$) Lagrangian is stationary with respect to variations of the λ_n^K (or $\lambda_n'^K$ for $\mathcal{L}'_K$) amplitudes. Stationarity with respect to the l_n^K (or r_n^K) amplitudes gives the eigenvalue problem from which the transition energies ω_K and the r_n^K (or l_n^K) amplitudes are computed. This eigenvalue problem consists of the right-hand (or left-hand) diagonalization of the EOM-CCSD similarity-transformed Hamiltonian matrix, which is usually performed using iterative techniques.[49−52] In the *gas phase*, the solution of this eigenvalue problem provides the excitation energies and eigenvectors of several states at once. Stationarity with respect to the Lagrangian multipliers gives the biorthonormality condition:

$$\langle \Phi^0 | L_K R_K | \Phi^0 \rangle = 1 \quad (10)$$

while stationarity with respect to the t_n amplitudes gives the equations for the λ_n^K (or $\lambda_n'^K$ for $\mathcal{L}'_K$) amplitudes. Finally, note that both Lagrangians are not functions of the reference molecular orbitals (MOs), which are kept frozen during the minimization procedure.

The two Lagrangian expressions are equivalent and provide the same values of energy, t_n, r_n^K, and l_n^K amplitudes. The Λ_K and Λ'_K operators are related by

$$\Lambda_K = \Lambda'_K + \Lambda''_K \quad (11)$$

where the amplitudes for Λ''_K are

$$\lambda_n''^K = \langle \Phi^0 | L_K R_K | \Phi^n \rangle \quad (12)$$

and Φ^n is an n-excited determinant.

In both formulations, the ground state Lagrangian is obtained with $L_0 = l_0^0 = 1$, $R_0 = r_0^0 = 1$, and $\Lambda_0 = \Lambda'_0 = \Lambda$:

$$\mathcal{L}_0 = \langle \Phi^0 | (1 + \Lambda) e^{-T} H e^T | \Phi^0 \rangle \quad (13)$$

Additionally, for an excited state K:

$$l_0^K = 0$$

$$r_0^K = -\sum_n \langle \Phi^0|\Lambda|\Phi^n\rangle\langle \Phi^n|R_K|\Phi^0\rangle \tag{14}$$

The expressions in eq 14 can be obtained from the biorthogonality condition between the ground state and the Kth excited state or by imposing the stationarity condition of the $\mathcal{L}_K$ (or $\mathcal{L}'_K$) Lagrangian with respect to r_0^K and l_0^K, respectively. Hence, the eigenvalue problem only includes the r_n^K and l_n^K amplitudes. When the two Lagrangians in eqs 1 and 2 are stationary with respect to variations of all of the parameters, one has

$$\mathcal{L}_K = \mathcal{L}'_K = E_K \tag{15}$$

I used the formulation in eqs 1 for the implementation of the EOM-CCSD analytic energy gradients in a development version of the Gaussian suite of programs,[53] since it requires a smaller number of terms due to the commutator.

2.2. State Specific PTED Scheme. As in the *gas phase*, the PCM Lagrangian also can be expressed in two equivalent ways:

$$\mathcal{G}_K^{\mathrm{PTED}} = \mathcal{L}_K + \frac{1}{2}\bar{\mathbf{V}}_K\cdot\bar{\mathbf{Q}}_K \tag{16}$$

$$\mathcal{G}'^{\mathrm{PTED}}_K = \mathcal{L}'_K + \frac{1}{2}\bar{\mathbf{V}}'_K\cdot\bar{\mathbf{Q}}'_K \tag{17}$$

where

$$\bar{\mathbf{V}}_K = \langle \Phi^0|L_K[e^{-T_K}\mathbf{V}e^{T_K}, R_K]|\Phi^0\rangle + \langle \Phi^0|(1+\Lambda_K)e^{-T_K}\mathbf{V}e^{T_K}|\Phi^0\rangle \tag{18}$$

$$\bar{\mathbf{Q}}_K = \langle \Phi^0|L_K[e^{-T_K}\mathbf{Q}e^{T_K}, R_K]|\Phi^0\rangle + \langle \Phi^0|(1+\Lambda_K)e^{-T_K}\mathbf{Q}e^{T_K}|\Phi^0\rangle \tag{19}$$

and

$$\bar{\mathbf{V}}'_K = \langle \Phi^0|L_K e^{-T_K}\mathbf{V}e^{T_K}R_K|\Phi^0\rangle + \langle \Phi^0|\Lambda'_K e^{-T_K}\mathbf{V}e^{T_K}|\Phi^0\rangle \tag{20}$$

$$\bar{\mathbf{Q}}'_K = \langle \Phi^0|L_K e^{-T_K}\mathbf{Q}e^{T_K}R_K|\Phi^0\rangle + \langle \Phi^0|\Lambda'_K e^{-T_K}\mathbf{Q}e^{T_K}|\Phi^0\rangle \tag{21}$$

The letter $\mathcal{G}$ is used to point out that the PCM Lagrangian has the status of a Gibbs free energy, since half of the solute−solvent interaction energy is spent to polarize the medium.[22,54] $\mathbf{V}$ and $\mathbf{Q}$ are the electrostatic potential and the reaction field operators on the boundary surface, respectively. The bold font for $\mathbf{V}$ and $\mathbf{Q}$ indicates that these are vectors of dimension equal to the number of surface elements in which the PCM cavity is partitioned.[46] The expectation values $\bar{\mathbf{V}}_K$ and $\bar{\mathbf{Q}}_K$ and $\bar{\mathbf{V}}'_K$ and $\bar{\mathbf{Q}}'_K$ depend on the total EOM-CCSD one particle density (without orbital relaxation).

Note that the subscript K appears on the T operators in eqs 18−21. In fact, the amplitudes for the T_K operators of the Kth excited state are not the same as those of the ground state. This is a consequence of the state specific formulation of the PCM Lagrangians, since the solvent interaction term couples the T_K with the R_K, L_K, and Λ_K (or Λ'_K) equations. For the same reason, the Lagrange multipliers ω_K and E_K lose their direct interpretation as transition energy and excited state energy, respectively.

Minimization of the Lagrangians with respect to variations of their parameters provides the equations to compute these parameters and evaluate the excited state free energy. At the end of the minimization, and similar to *gas phase* EOM-CCSD, both Lagrangians provide the same free energy, and the same solvent reaction field:

$$\bar{\mathbf{V}}_K = \bar{\mathbf{V}}'_K$$

$$\bar{\mathbf{Q}}_K = \bar{\mathbf{Q}}'_K \tag{22}$$

Additionally, the same relations between Λ_K and Λ'_K as in eqs 11 and 12 hold. Relations similar to those in eq 14 also hold for l_0^K and r_0^K. Although, for r_0^K, the Λ operator must be replaced by a $\Lambda_{(K)}$ operator, whose amplitudes are obtained by solving a set of linear equations formally similar to the PTED Λ equations in refs 25 and 28 except for the substitution $\bar{\mathbf{Q}} \rightarrow \bar{\mathbf{Q}}_K$. For the ground state ($K = 0$), the PTED free energy functional is recovered with $L_0 = l_0^0 = 1$, $R_0 = r_0^0 = 1$, $T_K = T$, and $\Lambda_0 = \Lambda'_0 = \Lambda$:

$$\mathcal{G}_0^{\mathrm{PTED}} = \mathcal{L}_0 + \frac{1}{2}\bar{\mathbf{V}}_0\cdot\bar{\mathbf{Q}}_0 \tag{23}$$

Transition energies in the PTED scheme can only be computed in a two-steps calculation as the difference between the K-th state and the ground state free energies.

Although the two formulations in eqs 16 and 17 are equivalent, only that in eq 16 is used in the following for the presentation and discussion of the working equations. The reason is that fewer terms are involved in eq 16 due to the commutator, and most of the computer code for *gas phase* EOM-CCSD can be reused. Consequently, the approximate free energy functionals introduced in section 2.3 will be derived from eq 16. Other approximate functionals could be derived from eq 17.[39] However, the equivalence between $\mathcal{G}_K^{\mathrm{PTED}}$ and $\mathcal{G}'^{\mathrm{PTED}}_K$ is lost in the corresponding approximations.

As mentioned above, the free energy for the Kth excited state can be computed by minimizing the Lagrangian in eq 16 with respect to t_n^K, r_n^K, l_n^K, λ_n^K, and ω_K. Before presenting the working equations, it is useful to separate the reference wave function contribution to $\mathcal{G}_K^{\mathrm{PTED}}$ from the rest. By introducing the normal-product form of an operator:[9]

$$X_N = X - \langle \Phi^0|X|\Phi^0\rangle = X - \bar{X}^0 \tag{24}$$

eq 16 can be rewritten as

$$\mathcal{G}_K^{\mathrm{PTED}} = \mathcal{G}^0 + \langle \Phi^0|L_K[e^{-T_K}H_N^{\mathrm{PCM}}e^{T_K}, R_K]|\Phi^0\rangle + \langle \Phi^0|(1+\Lambda_K)e^{-T_K}H_N^{\mathrm{PCM}}e^{T_K}|\Phi^0\rangle + \omega_K(1 - \langle \Phi^0|L_K R_K|\Phi^0\rangle) + \frac{1}{2}\bar{\mathbf{V}}_N^K\cdot\bar{\mathbf{Q}}_N^K \tag{25}$$

where $\mathcal{G}^0$ is the reference free energy:

$$\mathcal{G}^0 = \langle \Phi^0|H|\Phi^0\rangle + \frac{1}{2}\bar{\mathbf{V}}^0\cdot\bar{\mathbf{Q}}^0 \tag{26}$$

and H_N^{PCM} contains the PCM operator with the reference reaction field:

$$H_N^{\mathrm{PCM}} = H_N + V_N\cdot\bar{\mathbf{Q}}^0 \tag{27}$$

Here and in the following, I use the symmetry of the PCM kernel,[42,43] so that

$$\frac{\partial}{\partial\xi}\left(\frac{1}{2}\bar{\mathbf{V}}(\xi)\cdot\bar{\mathbf{Q}}(\xi)\right) = \bar{\mathbf{V}}^{\xi}(\xi)\cdot\bar{\mathbf{Q}}(\xi) \tag{28}$$

$$\frac{1}{2}\bar{\mathbf{V}}(\xi_1)\cdot\bar{\mathbf{Q}}(\xi_2) = \frac{1}{2}\bar{\mathbf{V}}(\xi_2)\cdot\bar{\mathbf{Q}}(\xi_1) \tag{29}$$

where the parameter ξ refers to the T_K, R_K, L_K, or Λ_K amplitudes. In the implementation, the symmetric version of the PCM equations[47] is used.

The partial derivative of $\mathcal{G}_K^{\mathrm{PTED}}$ with respect to λ_n^K gives the T_K equations:

$$\frac{\partial \mathcal{G}_K^{\mathrm{PTED}}}{\partial \lambda_n^K} = \langle \Phi^n | e^{-T_K} H_N^{\mathrm{PCM}} e^{T_K} | \Phi^0 \rangle + \langle \Phi^n | e^{-T_K} \mathbf{V}_N e^{T_K} | \Phi^0 \rangle \cdot \bar{\mathbf{Q}}_N^K = 0 \tag{30}$$

The coupling of the T_K equations with the excited state density is due to the presence of $\bar{\mathbf{Q}}_N^K$ in eq 30. Also, note the similarity of eq 30 with the T equations for the ground state PTED scheme.[25,28] The partial derivative of $\mathcal{G}_K^{PTED}$ with respect to ω_K gives the biorthonormality condition as in eq 10.

The partial derivative of $\mathcal{G}_K^{PTED}$ with respect to l_n^K gives the R_K and ω_K equations:

$$\begin{aligned}\frac{\partial \mathcal{G}_K^{PTED}}{\partial l_n^K} &= \langle \Phi^n | [e^{-T_K} H_N^{PCM} e^{T_K}, R_K] | \Phi^0 \rangle \\ &\quad + \langle \Phi^n | [e^{-T_K} \mathbf{V}_N e^{T_K}, R_k] | \Phi^0 \rangle \cdot \bar{\mathbf{Q}}_N^K \\ &\quad - \omega_K \langle \Phi^n | R_K | \Phi^0 \rangle \\ &= 0\end{aligned} \tag{31}$$

This is an eigenvalue problem, very similar to that of *gas phase* EOM-CCSD, and can be solved with the same techniques.[49−52] The equations for the L_K amplitudes are obtained from the partial derivative of $\mathcal{G}_K^{\mathrm{PTED}}$ with respect to r_n^K:

$$\begin{aligned}\frac{\partial \mathcal{G}_K^{\mathrm{PTED}}}{\partial r_n^K} &= \langle \Phi^0 | L_K [e^{-T_K} H_N^{\mathrm{PCM}} e^{T_K}, \tau_n] | \Phi^0 \rangle \\ &\quad + \langle \Phi^0 | L_K [e^{-T_K} \mathbf{V}_N e^{T_K}, \tau_n] | \Phi^0 \rangle \cdot \bar{\mathbf{Q}}_N^K \\ &\quad - \omega_K \langle \Phi^0 | L_K | \Phi^n \rangle \\ &= 0\end{aligned} \tag{32}$$

Finally, the equations for the Λ_K amplitudes are obtained from the partial derivative of $\mathcal{G}_K^{\mathrm{PTED}}$ with respect to t_n^K:

$$\begin{aligned}\frac{\partial \mathcal{G}_K^{\mathrm{PTED}}}{\partial t_n^K} &= \langle \Phi^0 | L_K [[e^{-T_K} H_N^{\mathrm{PCM}} e^{T_K}, \tau_n], R_K] | \Phi^0 \rangle \\ &\quad + \langle \Phi^0 | (1 + \Lambda_K) [e^{-T_K} H_N^{\mathrm{PCM}} e^{T_K}, \tau_n] | \Phi^0 \rangle \\ &\quad + \langle \Phi^0 | L_K [[e^{-T_K} \mathbf{V}_N e^{T_K}, \tau_n], R_K] | \Phi^0 \rangle \cdot \bar{\mathbf{Q}}_N^K \\ &\quad + \langle \Phi^0 | (1 + \Lambda_K) [e^{-T_K} \mathbf{V}_N e^{T_K}, \tau_n] | \Phi^0 \rangle \cdot \bar{\mathbf{Q}}_N^K \\ &= 0\end{aligned} \tag{33}$$

The nonlinear dependence of the solute−solvent interaction energy term in eq 25 from the EOM-CCSD reduced one particle density matrix (1PDM) couples eq 30−33, which must be simultaneously solved in order to compute $\mathcal{G}_K^{\mathrm{PTED}}$. At convergence, eq 25 reduces to

$$\mathcal{G}_K^{\mathrm{PTED}} = \mathcal{G}^0 + \Delta E_K^0 + \omega_K - \frac{1}{2} \bar{\mathbf{V}}_N^K \cdot \bar{\mathbf{Q}}_N^K \tag{34}$$

where

$$\Delta E_K^0 = \langle \Phi^0 | e^{-T_K} H_N^{\mathrm{PCM}} e^{T_K} | \Phi^0 \rangle + \langle \Phi^0 | e^{-T_K} \mathbf{V}_N e^{T_K} | \Phi^0 \rangle \cdot \bar{\mathbf{Q}}_N^K \tag{35}$$

The transition energy from the ground to the Kth excited state is then computed as the difference between $\mathcal{G}_K^{\mathrm{PTED}}$ in eq 34 and $\mathcal{G}_0^{\mathrm{PTED}}$ in eq 23.

2.3. Approximate Free Energy Functionals. The PTED scheme presented in section 2.2 is computationally expensive, since eqs 30−33 are coupled by the solvent reaction field. The approximations to eq 25 introduced in this section aim at decoupling the T and Λ_K equations from the R_K and L_K equations. This reduces the computational cost of the calculation and allows one to separate the ground state part of the calculation from the excited state part, as in the *gas phase*.

The first, obvious approximation is to neglect the $1/2 \bar{\mathbf{V}}_N^K \cdot \bar{\mathbf{Q}}_N^K$ term in eq 25. This corresponds to performing the EOM-CCSD calculation in the frozen reaction field of the reference function, which is usually not a good approximation for excited state calculations. Technically, this is a PTE scheme, since the solvent response does not depend on the correlation density. However, I will refer to it as FRF scheme (frozen-reaction-field) in the following since the name PTE will be used for another scheme proposed later in this section. The FRF scheme leaves the CCSD and EOM-CCSD equations unchanged compared to the *gas phase*, since the PCM contribution is only included in the MO coefficients and orbital energies. Therefore, I will not consider this approximation any further in this section, and I analyze its validity in the numerical tests in section 3.

The following approximations are named after the kind of CCSD-PCM ground state they can be related to: PTE, PTE(S), and PTES (where the S stands for singles).[25,28,32] If the reaction field $\bar{\mathbf{Q}}_N^K$ in eq 19 is split into three contributions:

$$\bar{\mathbf{Q}}_N^K = \tilde{\mathbf{Q}}_N^K + \tilde{\mathbf{Q}}_N^T + \tilde{\mathbf{Q}}_N^\Lambda \tag{36}$$

where

$$\tilde{\mathbf{Q}}_N^K = \langle \Phi^0 | L_K [e^{-T} \mathbf{Q}_N e^T, R_K] | \Phi^0 \rangle \tag{37}$$

$$\tilde{\mathbf{Q}}_N^T = \langle \Phi^0 | e^{-T} \mathbf{Q}_N e^T | \Phi^0 \rangle \tag{38}$$

$$\tilde{\mathbf{Q}}_N^\Lambda = \langle \Phi^0 | \Lambda_K e^{-T} \mathbf{Q}_N e^T | \Phi^0 \rangle \tag{39}$$

and a corresponding separation is introduced for $\bar{\mathbf{V}}_N^K$ in eq 18, the PCM term in $\mathcal{G}_K^{\mathrm{PTED}}$ in eq 25 can be written as

$$\begin{aligned}\frac{1}{2} \bar{\mathbf{V}}_N^K \cdot \bar{\mathbf{Q}}_N^K &= \frac{1}{2} \tilde{\mathbf{V}}_N^K \cdot \tilde{\mathbf{Q}}_N^K + \tilde{\mathbf{V}}_N^K \cdot \tilde{\mathbf{Q}}_N^T + \frac{1}{2} \tilde{\mathbf{V}}_N^T \cdot \tilde{\mathbf{Q}}_N^T \\ &\quad + \tilde{\mathbf{V}}_N^\Lambda \cdot \tilde{\mathbf{Q}}_N^T + \frac{1}{2} \tilde{\mathbf{V}}_N^\Lambda \cdot \tilde{\mathbf{Q}}_N^\Lambda + \tilde{\mathbf{V}}_N^\Lambda \cdot \tilde{\mathbf{Q}}_N^K\end{aligned} \tag{40}$$

The approximations described in the next three sections are based on neglecting selected contributions from eq 40.

2.3.1. PTE Free Energy Functional. In this scheme, the last five terms on the right-hand side of eq 40 are neglected. The corresponding free energy functional is

$$\begin{aligned}\mathcal{G}_K^{\mathrm{PTE}} &= \mathcal{G}^0 + \langle \Phi^0 | L_K [e^{-T} H_N^{\mathrm{PCM}} e^T, R_K] | \Phi^0 \rangle \\ &\quad + \langle \Phi^0 | (1 + \Lambda_K) e^{-T} H_N^{\mathrm{PCM}} e^T | \Phi^0 \rangle \\ &\quad + \omega_K (1 - \langle \Phi^0 | L_K R_K | \Phi^0 \rangle) + \frac{1}{2} \tilde{\mathbf{V}}_N^K \cdot \tilde{\mathbf{Q}}_N^K\end{aligned} \tag{41}$$

Minimizing eq 41 with respect to λ_n^K provides the T equations:

$$\frac{\partial \mathcal{G}_K^{\mathrm{PTE}}}{\partial \lambda_n^K} = \langle \Phi^n | e^{-T} H_N^{\mathrm{PCM}} e^T | \Phi^0 \rangle = 0 \tag{42}$$

which are the PTE equations for the ground state.[25,28] As anticipated above, this choice of neglected terms in eq 40 decouples the T equations from the excited state part of the calculation. The equations for the R_K and L_K amplitudes, obtained by minimization of eq 41 with respect to l_n^K and r_n^K, are the same as in eqs 31 and 32, except for the substitution $\bar{\mathbf{Q}}_N^K \rightarrow \tilde{\mathbf{Q}}_N^K$. The biorthonormality condition is obtained from the minimization of $\mathcal{G}_K^{\mathrm{PTE}}$ with respect to ω_K, see eq 10. Finally, the Λ_K equations are

$$\begin{aligned}\frac{\partial \mathcal{G}_K^{\mathrm{PTE}}}{\partial t_n} &= \langle \Phi^0 | L_K [[e^{-T} H_N^{\mathrm{PCM}} e^T, \tau_n], R_K] | \Phi^0 \rangle \\ &\quad + \langle \Phi^0 | L_K [[e^{-T} V_N e^T, \tau_n], R_K] | \Phi^0 \rangle \cdot \tilde{\mathbf{Q}}_N^K \\ &\quad + \langle \Phi^0 | (1 + \Lambda_K) [e^{-T} H_N^{\mathrm{PCM}} e^T, \tau_n] | \Phi^0 \rangle \\ &= 0 \end{aligned} \tag{43}$$

At convergence, eq 41 reduces to:

$$\begin{aligned}\mathcal{G}_K^{\mathrm{PTE}} &= \mathcal{G}^0 + \Delta E^0 + \omega_K - \frac{1}{2} \tilde{\mathbf{V}}_N^K \cdot \tilde{\mathbf{Q}}_N^K \\ &= \mathcal{G}_0^{\mathrm{PTE}} + \omega_K - \frac{1}{2} \tilde{\mathbf{V}}_N^K \cdot \tilde{\mathbf{Q}}_N^K \end{aligned} \tag{44}$$

where

$$\Delta E^0 = \langle \Phi^0 | e^{-T} H_N^{\mathrm{PCM}} e^T | \Phi^0 \rangle \tag{45}$$

and

$$\mathcal{G}_0^{\mathrm{PTE}} = \mathcal{G}^0 + \Delta E^0 \tag{46}$$

is the ground state PTE free energy. Therefore, the transition energy in this scheme can be computed in one step as

$$\Delta \mathcal{G}_K^{\mathrm{PTE}} = \mathcal{G}_K^{\mathrm{PTE}} - \mathcal{G}_0^{\mathrm{PTE}} \tag{47}$$

Although the ground state calculation is decoupled from the EOM part, the latter is still state specific, and only one excited state can be computed at a time. Additionally, since the T, R_K, and L_K equations do not depend on Λ_K (since the reaction field charges $\tilde{\mathbf{Q}}_N^K$ do not depend on Λ_K), it is not necessary to solve the Λ_K equations to compute $\mathcal{G}_K^{\mathrm{PTE}}$. The calculation of the Λ_K amplitudes is only necessary for the analytical gradients of $\mathcal{G}_K^{\mathrm{PTE}}$.

2.3.2. PTE(S) Free Energy Functional. The approximation introduced in the PTE(S) scheme is to neglect the last three terms in eq 40. The free energy functional in eq 25 becomes

$$\begin{aligned}\mathcal{G}_K^{\mathrm{PTE(S)}} &= \mathcal{G}^0 + \langle \Phi^0 | L_K [e^{-T} H_N^{\mathrm{PCM}} e^T, R_K] | \Phi^0 \rangle \\ &\quad + \langle \Phi^0 | (1 + \Lambda_K) e^{-T} H_N^{\mathrm{PCM}} e^T | \Phi^0 \rangle \\ &\quad + \omega_K (1 - \langle \Phi^0 | L_K R_K | \Phi^0 \rangle) + \frac{1}{2} \tilde{\mathbf{V}}_N^{TK} \cdot \tilde{\mathbf{Q}}_N^{TK} \end{aligned} \tag{48}$$

where

$$\begin{aligned}\tilde{\mathbf{V}}_N^{TK} &= \tilde{\mathbf{V}}_N^K + \tilde{\mathbf{V}}_N^T \\ \tilde{\mathbf{Q}}_N^{TK} &= \tilde{\mathbf{Q}}_N^K + \tilde{\mathbf{Q}}_N^T \end{aligned} \tag{49}$$

The T equations are the same as those of the PTE scheme in eq 42. The equations for the R_K and L_K amplitudes are formally similar to the PTED equations in eqs 31 and 32 with the substitution $\bar{\mathbf{Q}}_N^K \rightarrow \tilde{\mathbf{Q}}_N^{TK}$. The Λ_K equations are, on the other hand,

$$\begin{aligned}\frac{\partial \mathcal{G}_K^{\mathrm{PTE(S)}}}{\partial t_n} &= \langle \Phi^0 | L_K [[e^{-T} H_N^{\mathrm{PCM}} e^T, \tau_n], R_K] | \Phi^0 \rangle \\ &\quad + \langle \Phi^0 | (1 + \Lambda_K) [e^{-T} H_N^{\mathrm{PCM}} e^T, \tau_n] | \Phi^0 \rangle \\ &\quad + \langle \Phi^0 | L_K [[e^{-T} \mathbf{V}_N e^T, \tau_n], R_K] | \Phi^0 \rangle \cdot \tilde{\mathbf{Q}}_N^{TK} \\ &\quad + \langle \Phi^0 | e^{-T} \mathbf{V}_N e^T | \Phi^n \rangle \cdot \tilde{\mathbf{Q}}_N^{TK} \\ &= 0 \end{aligned} \tag{50}$$

At convergence, $\mathcal{G}_K^{\mathrm{PTE(S)}}$ in eq 38 reduces to

$$\mathcal{G}_K^{\mathrm{PTE(S)}} = \mathcal{G}_0^{\mathrm{PTE(S)}} + \omega_K - \frac{1}{2} \tilde{\mathbf{V}}_N^K \cdot \tilde{\mathbf{Q}}_N^K \tag{51}$$

where

$$\mathcal{G}_0^{\mathrm{PTE(S)}} = \mathcal{G}^0 + \Delta E^0 + \frac{1}{2} \tilde{\mathbf{V}}_N^T \cdot \tilde{\mathbf{Q}}_N^T \tag{52}$$

is the ground state PTE(S) free energy,[32] and ΔE^0 is defined in eq 45. Similar to the PTE scheme, the ground state calculation is decoupled from the excited state part, and the Λ_K equations in eq 50 only need to be solved for computing analytic gradients of $\mathcal{G}_K^{\mathrm{PTE(S)}}$. Therefore, ground and excited state calculations can be performed in one step for each Kth excited state with the PTE(S) scheme as well.

2.3.3. PTES Free Energy Functional. In the PTES scheme, only the terms in the PCM contribution to the free energy functional in eq 25 that strictly couple the T, R_K–L_K, and Λ_K equations are neglected. These are the last two terms in eq 40. Thus, the PTES free energy functional is

$$\begin{aligned}\mathcal{G}_K^{\mathrm{PTES}} &= \mathcal{G}^0 + \langle \Phi^0 | L_K [e^{-T} H_N^{\mathrm{PCM}} e^T, R_K] | \Phi^0 \rangle \\ &\quad + \langle \Phi^0 | (1 + \Lambda_K) e^{-T} H_N^{\mathrm{PCM}} e^T | \Phi^0 \rangle \\ &\quad + \omega_K (1 - \langle \Phi^0 | L_K R_K | \Phi^0 \rangle) + \frac{1}{2} \tilde{\mathbf{V}}_N^{TK} \cdot \tilde{\mathbf{Q}}_N^{TK} \\ &\quad + \tilde{\mathbf{V}}_N^{\Lambda} \cdot \tilde{\mathbf{Q}}_N^T \end{aligned} \tag{53}$$

The T equations are

$$\begin{aligned}\frac{\partial \mathcal{G}_K^{\mathrm{PTES}}}{\partial \lambda_n^K} &= \langle \Phi^n | e^{-T} H_N^{\mathrm{PCM}} e^T | \Phi^0 \rangle + \langle \Phi^n | e^{-T} \mathbf{V}_N e^T | \Phi^0 \rangle \cdot \tilde{\mathbf{Q}}_N^T \\ &= 0 \end{aligned} \tag{54}$$

which are the ground state PTES T equations.[32] The R_K and L_K equations are the same as the PTE(S) scheme in section 2.3.2. The Λ_K equations are

$$\begin{aligned}\frac{\partial \mathcal{G}_K^{\mathrm{PTES}}}{\partial t_n} &= \langle \Phi^0 | L_K [[e^{-T} H_N^{\mathrm{PCM}} e^T, \tau_n], R_K] | \Phi^0 \rangle \\ &\quad + \langle \Phi^0 | (1 + \Lambda_K) [e^{-T} H_N^{PCM} e^T, \tau_n] | \Phi^0 \rangle \\ &\quad + \langle \Phi^0 | L_K [[e^{-T} \mathbf{V}_N e^T, \tau_n], R_K] | \Phi^0 \rangle \cdot \tilde{\mathbf{Q}}_N^{TK} \\ &\quad + \langle \Phi^0 | \Lambda_K [e^{-T} \mathbf{V}_N e^T, \tau_n] | \Phi^0 \rangle \tilde{\mathbf{Q}}_N^T \\ &\quad + \langle \Phi^0 | e^{-T} \mathbf{V}_N e^T | \Phi^n \rangle \cdot \bar{\mathbf{Q}}_N^K \\ &= 0 \end{aligned} \tag{55}$$

At convergence, $\mathcal{G}_K^{\mathrm{PTES}}$ in eq 53 reduces to

$$\mathcal{G}_K^{\mathrm{PTES}} = \mathcal{G}_0^{\mathrm{PTES}} + \omega_K - \frac{1}{2} \tilde{\mathbf{V}}_N^K \cdot \tilde{\mathbf{Q}}_N^K \tag{56}$$

where

dx.doi.org/10.1021/ct300382a | J. Chem. Theory Comput. 2012, 8, 5081−5091

$$\mathcal{G}_0^{\mathrm{PTES}} = \mathcal{G}^0 + \Delta E^0 + \frac{1}{2}\tilde{\mathbf{V}}_N^T \cdot \tilde{\mathbf{Q}}_N^T \tag{57}$$

and ΔE^0 is defined in eq 45. Although eqs 56 and 57 look the same as eqs 51 and 52, $\mathcal{G}_K^{\mathrm{PTES}} \neq \mathcal{G}_K^{\mathrm{PTE(S)}}$ since the T amplitudes are computed with different equations (eq 54 and eq 42, respectively). Thus, the R_K and L_K amplitudes and the solvent reaction field are also different for the two schemes.

Also in the PTES scheme, the T equations are decoupled from the R_K and L_K equations, which in turn are decoupled from the Λ_K equations. The latter need to be solved only for analytic gradients of $\mathcal{G}_K^{\mathrm{PTES}}$ with respect to an external perturbation. Although the entire $\bar{\mathbf{Q}}_N^K$ charges appear in the last term of eq 55, only the $\tilde{\mathbf{Q}}_N^\Lambda$ part (see eqs 36 and 39) changes during the iterative solution of eq 55, while the $\tilde{\mathbf{Q}}_N^T$ and $\tilde{\mathbf{Q}}_N^K$ contributions (see eqs 37 and 38) are fixed, as they come from the solution of the PTES T, R_K, and L_K equations.

2.4. Implementation. In this section, the explicit form of the PCM terms of the PTED functional that appear in eqs 30−33 is reported. The expressions for the remaining terms are those of *gas phase* EOM-CCSD and can be found in the literature.[4] The PCM terms for the approximated functionals introduced in section 2.3 can be derived from the following expressions with the proper choice of the reaction field charges.

The PCM terms in eq 30 for the T equations are exactly the same as those for the ground state PTED[25] approach when the $\bar{\mathbf{Q}}_N$ are replaced by $\bar{\mathbf{Q}}_N^K$. Indeed, the same code can be directly reused provided that the correct set of charges is employed. On the other hand, new terms need to be added to the EOM code. These are, for the R_K equations,

$$r_i^a\colon [-r_k^a v_{ki} + r_i^c v_{ca} + v_{kc}(r_{ik}^{ac} - r_k^a t_i^c - r_i^c t_k^a)] \cdot \bar{\mathbf{Q}}_N^K \tag{58}$$

$$r_{ij}^{ab}\colon [P(ab)(r_{ij}^{ac}(v_{cb} - v_{kc}t_k^b) - t_{ij}^{ac} v_{kc} r_k^b) - P(ij)(r_{ik}^{ab}(v_{kj} + v_{kc}t_j^c) + t_{ik}^{ab} v_{kc} r_j^c)] \cdot \bar{\mathbf{Q}}_N^K \tag{59}$$

The operator $P(pq)$ antisymmetrizes the indexes p and q. The indexes i, j, etc. refer to occupied MOs; a, b, etc. refer to virtual MOs; and p, q, etc. refer to general MOs. Equation 58 contains the PCM terms in the singles R_K equation, while eq 59 contains the terms in the doubles R_K equations. Similarly, the PCM terms in the singles and doubles L_K equations are, respectively

$$l_a^i\colon \left[-l_a^k(v_{ki} + t_k^c v_{ic}) + l_c^i(v_{ca} - t_k^c v_{ka}) - \frac{1}{2} t_{kl}^{cd}(l_{cd}^{il} v_{ka} + l_{ad}^{kl} v_{ic})\right] \cdot \bar{\mathbf{Q}}_N^K \tag{60}$$

$$l_{ab}^{ij}\colon [P(ij, ab) v_{ia} l_b^j + P(ab) l_{ac}^{ij}(v_{cb} - v_{kb}t_k^c) - P(ij) l_{ab}^{ik}(v_{kj} + v_{jc}t_k^c)] \cdot \bar{\mathbf{Q}}_N^K \tag{61}$$

where $P(ij,ab) = P(ij)P(ab)$.

The Λ_K equations in eq 33 include many common terms with the ground state PTED Λ equations (fourth term on the right-hand side of eq 33)[25,28] and some new terms (third term on the right-hand side of eq 33). The new terms are

$$\lambda_a^i\colon \left[-r_k^c(l_a^k v_{ic} + l_c^i v_{ka}) - \frac{1}{2} r_{kl}^{cd}(l_{cd}^{il} v_{ka} + l_{ad}^{kl} v_{ic})\right] \cdot \bar{\mathbf{Q}}_N^K \tag{62}$$

$$\lambda_{ab}^{ij}\colon [-P(ab) l_{ac}^{ij} v_{kb} r_k^c - P(ij) l_{ab}^{ik} v_{jc} r_k^c] \cdot \bar{\mathbf{Q}}_N^K \tag{63}$$

Although some terms in eqs 58−63 scale as $O(N^5)$, where N is the number of basis functions, they can be folded in intermediates already computed for the regular EOM-CCSD calculation. Therefore, the extra work introduced by these PCM terms is negligible. A relatively expensive part of the EOM-CCSD-PCM calculation is the evaluation of the reduced 1PDM, necessary for the computation of the reaction field $\bar{\mathbf{Q}}_N^K$. The expression of the 1PDM for the Kth state is

$$\bar{\gamma}_{pq}^K = \langle \Phi^0 | L_K [e^{-T}\{p^\dagger q\} e^T, R_K] | \Phi^0 \rangle + \langle \Phi^0 | (1 + \Lambda_K) e^{-T}\{p^\dagger q\} e^T | \Phi^0 \rangle \tag{64}$$

The scaling for the evaluation of eq 64 is $O(N^5)$, which is smaller than the scaling of the leading terms in eqs 30−33, i.e. $O(N^6)$. Additionally, the reaction field can be updated once every several cycles of eqs 30−33, so that the extra work related to eq 64 is not significant.

The real cost of an EOM-CCSD-PCM-PTED calculation is due to the coupling of eqs 30−33, and to the state-specific nature of the method. The former issue implies the solution of eq 33 even in a single point energy calculation, contrary to *gas phase* EOM-CCSD, and requires several PCM macroiterations until convergence in the reaction field. The latter issue prevents a multistate calculation, typical of *gas phase* EOM-CCSD, since the same reaction field is applied to all of the intermediate eigenvalues of the similarity-transformed Hamiltonian. This extra computational effort compared to *gas phase* EOM-CCSD is less relevant in geometry optimizations, since the Λ_K vector is always necessary for the evaluation of the analytic energy gradients, and one electronic state is considered at a time. Further savings are obtained through the approximated functionals presented in section 2.3.

All of the free energy functionals and corresponding analytic gradients are implemented for restricted closed-shell and unrestricted wave functions with and without frozen core MOs, and make full use of Abelian point group symmetry.

2.5. Analytic Energy Gradients. Exploring potential energy surfaces requires the evaluation of forces on the molecular nuclei. Analytic energy gradients are the most efficient way to compute forces and to reduce numerical noise. The latter is an important issue for excited state calculations, where a numerical evaluation of the forces (performed with numerical differentiation of the energy computed at displaced positions of the nuclei) can incur severe errors if a nucleus displacement is accompanied by an undetected shift in the order of the states.

Therefore, I implemented analytic energy gradients for all of the functionals presented in this work, eqs 25, 41, 48, and 53. When the t, r_K, l_K, and λ_K amplitudes are computed, each functional is minimized with respect to variations in all of the amplitudes. Thus, only the derivatives of the MO coefficients, the atomic orbitals (AOs), and the PCM cavity with respect to the motion of the nuclei need to be evaluated.

The presence of PCM adds few extra terms to the *gas phase* EOM-CCSD energy gradient expressions.[5−7] Furthermore, these terms are very similar to the ground state case for PTED and PTE(S). For the PTE scheme, the PCM terms are similar to those of PTED. Since the same expressions of the PCM terms in the ground state methods can be used for the corresponding excited state methods when the proper density and reaction field are substituted, I do not repeat these expressions here. Instead, the replacement of the ground state

Table 1. List of Replacements of the Ground State Reaction Field and Reduced 1PDM with the Corresponding Excited State Quantities, for the EOM-CCSD-PCM Analytic Gradients of the PTED, PTE, and PTE(S) Functionals in eqs 25, 41, and 48

PTED	$\bar{\mathbf{Q}}_N^0 \rightarrow \bar{\mathbf{Q}}_N^K$	$\bar{\gamma}_{pq}^0 \rightarrow \bar{\gamma}_{pq}^K$
PTE	$\bar{\mathbf{Q}}_N^0 \rightarrow \tilde{\mathbf{Q}}_N^K$	$\bar{\gamma}_{pq}^0 \rightarrow \tilde{\gamma}_{pq}^K$
PTE(S)	$\tilde{\mathbf{Q}}_N^T \rightarrow \tilde{\mathbf{Q}}_N^{TK}$	$\tilde{\gamma}_{pq}^T \rightarrow \tilde{\gamma}_{pq}^{TK}$

1PDM and $\bar{\mathbf{Q}}_N$[25,28] with their corresponding excited state counterparts are summarized in Table 1. A partition of $\bar{\gamma}_{pq}^K$ (eq 64) as in eq 36 is applied in Table 1.

The gradients of the PCM terms in the PTES functional in eq 53 are slightly more complicated than those of the corresponding ground state method. The PTES energy term in eq 53 can be recast as the linear combination of three terms quadratic in some density:

$$\frac{1}{2}\tilde{\mathbf{V}}_N^{TK}\cdot\tilde{\mathbf{Q}}_N^{TK} + \tilde{\mathbf{V}}_N^{\Lambda}\cdot\tilde{\mathbf{Q}}_N^{T} = \frac{1}{2}\bar{\mathbf{V}}_N^{K}\cdot\bar{\mathbf{Q}}_N^{K} + \frac{1}{2}\tilde{\mathbf{V}}_N^{K}\cdot\tilde{\mathbf{Q}}_N^{K} - \frac{1}{2}\tilde{\mathbf{V}}_N^{\Lambda K}\cdot\tilde{\mathbf{Q}}_N^{\Lambda K} \quad (65)$$

The gradients of the expression on the right-hand side of eq 65 can then be obtained by reusing the code for the PTED scheme (first row in Table 1) and looping three times with the $\bar{\gamma}_{pq}^K$, $\tilde{\gamma}_{pq}^K$, and $\tilde{\gamma}_{pq}^{\Lambda K}$ densities.

Although extra terms appear in the EOM-CCSD-PCM analytic energy gradients, their computational cost is negligible compared to the evaluation of the reduced two particle density matrix (2PDM), which is necessary even in *gas phase* EOM-CCSD.

3. NUMERICAL APPLICATIONS

This section contains numerical results for two widely studied molecules: *trans*-acrolein and methylencyclopropene (MCP),[40,55−65] see Figure 1. The scope of these examples is

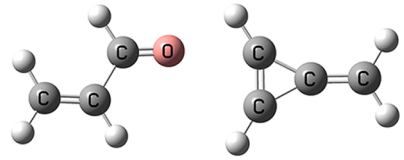

Figure 1. Structures of *trans*-acrolein and MCP.

to compare the methods described in section 2 and provide some information about their behavior. Vertical and adiabatic transition energies are reported. However, the former are not directly comparable to experimental data because the equilibrium solvation regime is used in this work. The optimized geometries of all of the species in gas and in solution can be found in the Supporting Information.

Initially, the configuration interaction singles (CIS) method is used to identify and characterize the PES stationary points for all of the electronic excited states, in gas and in solution. Analytic second derivatives of the CIS energy are employed for computing the harmonic vibrational frequencies at the stationary points to distinguish minima from saddle points. These optimized geometries are then used as starting points for the EOM-CCSD optimizations. The aug-cc-pVDZ[66] basis set is used throughout the section. The PCM cavity is built from spheres centered on the nuclei with universal force field (UFF) atomic radii:[67] 1.925 Å for C, 1.750 Å for O, and 1.443 Å for H, scaled for a factor of 1.1. The UFF radii are chosen because of their availability for most of the periodic table, whereas the scaling factor of 1.1 provides a cavity with a surface close to the solvent excluded surface.[46] All of the calculations are performed with a development version of the Gaussian suite of programs.[53]

3.1. *trans*-Acrolein. For *trans*-acrolein, water and cyclohexane are considered as solvents (ε = 78.4 and 2, respectively). The ground state of this molecule is planar with C_s symmetry in all phases, see Figure 1a. The first two excited states are analyzed. The first transition is $n \rightarrow \pi^*$ to an A″ state. The optimized geometry of this state is still planar in all phases. The second transition is $\pi \rightarrow \pi^*$ to an A′ state. For this state, the stationary point at the planar geometry is a first order saddle point in all phases. CIS finds a minimum at a distorted geometry in the *gas phase*, with a dihedral angle of 160° for the OCCC frame. The hydrogens of the CH_2 group are out-of-plane with CCCH dihedral angles of −50° and 137°, respectively. Minima of similar structure are also found in water and cyclohexane. However, EOM-CCSD does not find such minima, and the CH_2 group rotates until it is almost orthogonal to the OCCC frame. Unfortunately, at that point, following the original excited state becomes difficult due to the breaking of π conjugation and mixing of the ground and excited states. A detailed analysis of this complicated electronic structure is beyond the scope of this work, and I limited the focus on the structure constrained in planar geometry (first order saddle point).

The vertical transition energies for the two electronic states, computed with the schemes presented in section 2, are shown in Figure 2. The *gas phase* energies are shown as straight lines

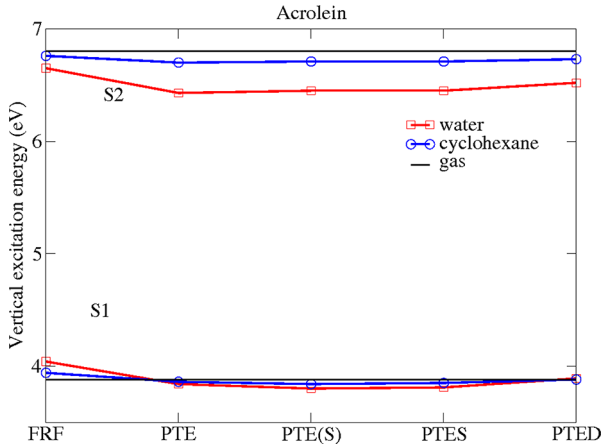

Figure 2. Acrolein vertical excitation energies (eV) in the equilibrium solvation regime. The *gas phase* values are reported as straight lines for reference.

for reference. The optimized ground state geometries obtained with the PTE, PTE(S), PTES, and PTED schemes are all very similar, so the shift in energies is mainly due to the EOM-CCSD calculations. The first transition is not very sensitive to the solvent effect, as the PTED results indicate. However, the PTED energies are computed as the difference between two separate calculations for the ground and the excited states, see section 2.2. Therefore, a small solvent effect on the excitation

energy means that such an effect is similar for the ground and the excited states. This may not be the case when the nonequilibrium solvation regime is used, as already shown in ref 65. In fact, for polar solvents, the optical dielectric constant (ε_∞) used in nonequilibrium calculations is much smaller than the static dielectric constant (ε) used in the ground state calculation. The approximate PTE, PTE(S), and PTES schemes reproduce the PTED results fairly closely, contrary to the FRF scheme, which provides a difference of 0.15 eV for water.

The second transition is more sensitive to the solvent effect. The $\pi\rightarrow\pi^*$ character indicates a larger charge separation of the electronic density in the excited state, which is more stabilized by a polar solvent. Indeed, Figure 2 shows a lower excitation energy in water. Also in this case, the approximate schemes are quite close to the PTED results, with differences of 0.07 eV in water for PTE(S) and PTES and 0.09 for PTE. The FRF difference is again quite large: 0.23 eV. A similar trend is shown by the cyclohexane results, although less marked due to the low polarity of this solvent.

The results for the adiabatic transition energy calculations are shown in Figure 3. The data are reported as an energy shift

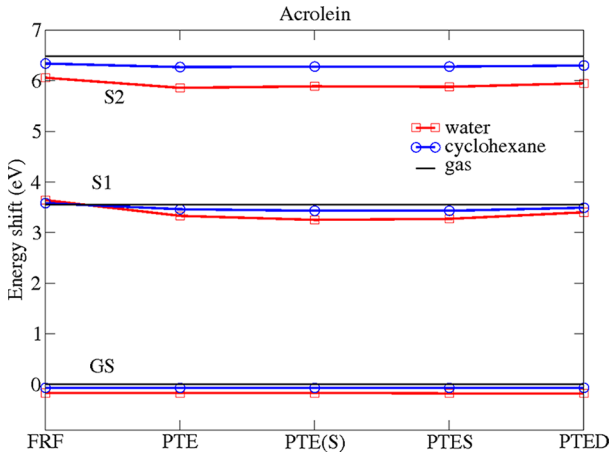

Figure 3. Acrolein adiabatic energy shifts (eV) from the *gas phase* ground state energy. The *gas phase* values are reported as straight lines for reference.

from the *gas phase* ground state energy, in order to show the solvent effect on the ground as well as the excited states. The solvent stabilizes the ground state energy of 0.07 eV for cyclohexane and 0.17−0.18 eV for water with all of the PCM schemes. A similar stabilization is reported for the first excited state with all of the schemes, except FRF. For the latter, the energy of the excited states in solution is higher than that in the *gas phase*, which is qualitatively wrong. Note that the shift of the water adiabatic transition energy from the *gas phase* value is 0.03 eV, which is in qualitative agreement with CASSCF and CASPT2 results (0.14 and 0.18 eV, respectively),[63] contrary to the results obtained with SAC−CI (−0.03 eV).[40] The adiabatic transition energy of the second excited state is again more sensitive to the presence of the solvent than that of the first excited state. In fact, the adiabatic transition energy for this state is 0.39 eV lower than the vertical transition energy, compared to the 0.31 eV for the first excited state. The PTE, PTE(S), and PTES results are 0.07−0.13 eV lower than the PTED result for the first transition energy in water and 0.06−0.09 eV for the second transition energy. The differences with the FRF scheme are 0.24 and 0.19 eV for the first and second transition energies, respectively. Better agreement is obtained with cyclohexane due to its low polarity.

3.2. Methylencyclopropene (MCP). MCP has a planar structure of C_{2v} symmetry in the ground state for all of the phases, see Figure 1b. Only the first excited state is considered (B_2 symmetry), and the solvents are methanol and *n*-pentane (ε = 32.6 and 1.8, respectively). The CIS geometry optimization of the first excited state was initially performed with a C_{2v} symmetry constraint. The stationary point is a second order saddle point (two imaginary frequencies). Moving along the normal mode with the largest imaginary frequency, a minimum of C_2 symmetry is found, while moving along the other normal mode with imaginary frequency leads to a first order saddle point of C_s symmetry. The latter connects the two symmetrical C_2 minima. A representation of the C_2 and C_s stationary points is shown in Figure 4. EOM-CCSD finds similar stationary points in all phases.

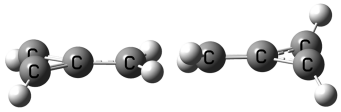

Figure 4. Structures of the MCP nonplanar stationary points on the first excited state PES. The C_s structure is a first order saddle point, while the C_2 structure is a minimum.

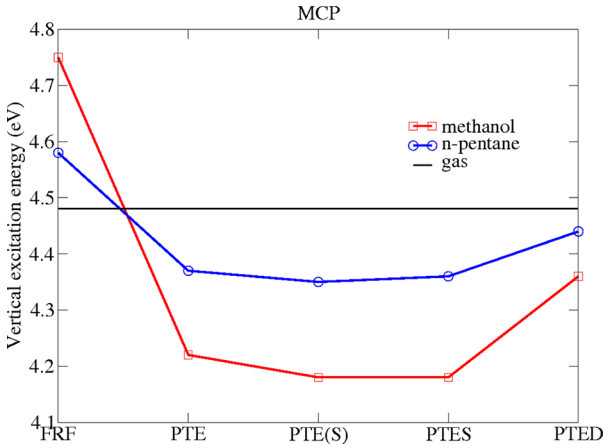

Figure 5. MCP vertical excitation energies (eV) in the equilibrium solvation regime. The *gas phase* value is reported as a straight line for reference.

The vertical excitation energies are reported in Figure 5. Both solvents produce an energy red shift, except with the FRF scheme. Also in this case, this approximation produces qualitatively wrong results. The PTE, PTE(S), and PTES approximations overcorrect this behavior, and the difference with PTED is now on the order of 0.12−0.16 eV for methanol and 0.07−0.09 eV for *n*-pentane. However, these schemes reproduce the same trend as the PTED scheme.

The adiabatic transition energies for the three stationary points on the PES of this excited state are shown in Figure 6. The ground state is 0.11 eV more stable in methanol and 0.04 eV in *n*-pentane than in the gas phase with all of the PCM schemes. The adiabatic transition energies, on the other hand, are more sensitive to the choice of the PCM scheme. PTED shows a small red shift of the adiabatic transition energy

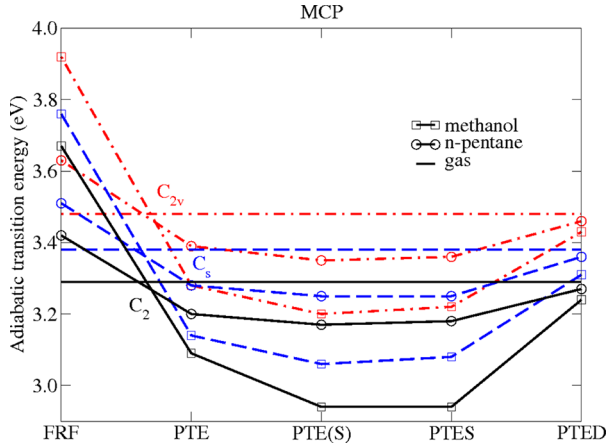

Figure 6. MCP adiabatic transition energies (eV) for the three stationary points on the first excited state PES. C_{2v} indicates the second order saddle point, C_s the first order saddle point, and C_2 the minimum. The *gas phase* values are reported as straight lines for reference.

compared to the *gas phase* for all of the optimized structures (0.05 eV for the C_{2v} and C_2 structures and 0.07 eV for the C_s structure in methanol, 0.02 eV for all the structures in *n*-pentane). The FRF scheme provides a rather large blue shift (0.38−0.44 eV in methanol and 0.13−1.15 eV in *n*-pentane). The PTE scheme, which is the closest to PTED, provides a 0.20−0.24 eV red shift in methanol and 0.09−0.10 eV red shift in *n*-pentane. The PTE(S) and PTES provide similar results with red shifts on the order of 0.26−0.35 eV in methanol and 0.11−0.13 eV in *n*-pentane. Therefore, also for the adiabatic transition energies, the FRF trend is opposite to all of the other methods, while the other three approximate schemes recover the right trend but overestimate the correction.

4. DISCUSSION AND CONCLUSIONS

In this work, I present the expressions for computing the energy and the analytic energy gradients for electronic excited states of molecules in solution through the coupling of the EOM-CCSD and PCM methods in a state-specific free energy Lagrangian formulation. Three approximations of the complete model are also introduced. The complete model, PTED, couples the ground state T equations and the excited state R_K, L_K, and Λ_K equations through the PCM energy contribution, which is nonlinear in the EOM-CCSD reduced 1PDM. The approximate schemes, PTE, PTE(S), and PTES, decouple the ground state equations from the excited state part similar to *gas phase* EOM-CCSD. The decoupling is achieved by neglecting selected contributions to the PCM energy term, according to the corresponding ground state CCSD-PCM schemes.[25,28,32] A fourth approximate scheme is also possible, where the PCM term in the CC part is completely neglected and the solvent contribution is only introduced at the reference wave function level. This corresponds to a PTE scheme for the ground state, but here it is called FRF (for frozen-reaction-field) to distinguish it from the PTE scheme presented in section 2.3.1.

The five schemes discussed in section 2 are tested on two molecules: *trans*-acrolein and MCP, each in two solvents of different polarity. Results for vertical and adiabatic transition energies are reported in section 3. However, the vertical excitation energies are computed in the equilibrium solvation regime and, thus, are not directly comparable to experimental results. In fact, in this regime, the time scale of the response of the solvent molecules is assumed similar to the time scale of the changes in the solute density. This is obviously not a good assumption for a fast vertical excitation process, while it is valid for geometrical relaxations of the solute molecule, and thus for adiabatic transition energies. The nonequilibrium regime can be modeled with PCM,[22] and its extension to the EOM-CCSD-PCM schemes will be the subject of a future publication.

The results in section 3 show that the FRF scheme is often qualitatively wrong, since blue shifts in both vertical and adiabatic transition energies are obtained, opposite to all of the other schemes (compare Figures 2 and 3 and Figures 5 and 6). The PTE, PTE(S), and PTES schemes correct this behavior, although the magnitude of this correction can be very large, as shown in the MCP case (Figures 5 and 6). The more approximate PTE scheme is in slightly better agreement with PTED, probably for a fortuitous cancellation of errors. However, further experience with these methods is necessary to confirm this trend. Small differences are found between the PTE(S) and PTES results.

The computational costs of PTE, PTE(S), and PTES are similar, since the cost of the extra PCM terms introduced in the EOM equations are negligible compared to the *gas phase* EOM-CCSD terms (see discussion in section 2.4). All three are more expensive than the FRF scheme, since PCM iterations are necessary for the solution of the EOM equations, and only one state at a time can be computed. However, the results in this work clearly show that the FRF scheme is not reliable. PTED is the most expensive scheme, due to the coupling of eqs 30−33. The relative cost of PTED is attenuated in geometry optimization calculations compared to PTE, PTE(S), and PTES since the Λ_K vector, eq 33, is necessary for evaluating the energy gradients for all of the schemes. Although, eqs 30 and 33 still need to be solved several times for each PTED energy evaluation. The extra effort introduced by the coupling of eqs 30−33 in the PTED scheme is more evident for vertical transition calculations, since no energy gradient evaluations are required. Moreover, the PTED vertical transition energy requires two separate calculations since it is computed as the difference between the excited state and the ground state energy. On the other hand, the vertical transition energy is obtained in a single calculation with the approximate schemes thanks to the decoupling of the ground state T equations from the excited state part.

In conclusion, the combination of EOM-CCSD and PCM opens the possibility of accurately studying the excited state electronic structure of solvated systems and exploring their potential energy surface. Furthermore, with the extension to the nonequilibrium regime, it will be possible to simulate absorption as well as emission spectra, thus completely characterizing the photophysical properties of molecules in the condensed phase.

■ ASSOCIATED CONTENT

Supporting Information

The optimized geometries of *trans*-acrolein and MCP, in the gas phase and in solution, for all of the EOM-CCSD-PCM and CCSD-PCM schemes are reported. This material is available free of charge via the Internet at http://pubs.acs.org.

■ AUTHOR INFORMATION

Corresponding Author

*E-mail: marco@gaussian.com.

Notes

The authors declare no competing financial interest.

■ ACKNOWLEDGMENTS

I wish to thank Dr. Giovanni Scalmani and Dr. Fernando R. Clemente for useful discussions.

■ REFERENCES

(1) Schlegel, H. B. *J. Comput. Chem.* **1982**, *3*, 214−218.
(2) Hratchian, H. P.; Schlegel, H. B. Finding Minima, Transition States, and Following Reaction Pathways on Ab Initio Potential Energy Surfaces. In *Theory and Applications of Computational Chemistry: The First Forty Years*; Dykstra, C. E., Frenking, G., Kim, K. S., Scuseria, G. E., Eds.; Elsevier: Amsterdam, The Netherlands, 2005; pp 195−249.
(3) Schlegel, H. B. *WIREs Comput. Mol. Sci.* **2011**, *1*, 790−809.
(4) Stanton, J. F.; Bartlett, R. J. *J. Chem. Phys.* **1993**, *98*, 7029−7039.
(5) Stanton, J. F. *J. Chem. Phys.* **1993**, *99*, 8840−8847.
(6) Stanton, J. F.; Gauss, J. *J. Chem. Phys.* **1994**, *100*, 4695−4698.
(7) Kallay, M.; Gauss, J. *J. Chem. Phys.* **2004**, *121*, 9257−9269.
(8) Bartlett, R. J.; Musial, M. *Rev. Mod. Phys.* **2007**, *79*, 291−352.
(9) Shavitt, I.; Bartlett, R. J. *Many-Body Methods in Chemistry and Physics*; Cambridge University Press: Cambridge, United Kingdom, 2009.
(10) Osted, A.; Kongsted, J.; Mikkelsen, K. V.; Christiansen, O. *J. Phys. Chem. A* **2004**, *108*, 8646−8658.
(11) Kongsted, J.; Osted, A.; Pedersen, T. B.; Mikkelsen, K. V.; Christiansen, O. *J. Phys. Chem. A* **2004**, *108*, 8624−8632.
(12) Aidas, K.; Kongsted, J.; Osted, A.; Mikkelsen, K. V.; Christiansen, O. *J. Phys. Chem. A* **2005**, *109*, 8001−8010.
(13) Kowalski, K.; Valiev, M. *J. Phys. Chem. A* **2006**, *110*, 13106−13111.
(14) Fan, P.-D.; Valiev, M.; Kowalski, K. *Chem. Phys. Lett.* **2008**, *458*, 205−209.
(15) Day, P. N.; Jensen, J. H.; Gordon, M. S.; Webb, S. P.; Stevens, W. J.; Krauss, M.; Garmer, D.; Basch, H.; Cohen, D. *J. Chem. Phys.* **1996**, *105*, 1968−1986.
(16) Gordon, M. S.; Freitag, M. A.; Bandyopadhyay, P.; Jensen, J. H.; Kairys, V.; Stevens, W. J. *J. Phys. Chem. A* **2001**, *105*, 293−307.
(17) Bandyopadhyay, P.; Gordon, M. S.; Mennucci, B.; Tomasi, J. *J. Chem. Phys.* **2002**, *116*, 5023−5032.
(18) Sneskov, K.; Schwabe, T.; Kongsted, J.; Christiansen, O. *J. Chem. Phys.* **2011**, *134*, 104108.
(19) Slipchenko, L. V. *J. Phys. Chem. A* **2010**, *114*, 8824−8830.
(20) Kosenkov, D.; Slipchenko, L. V. *J. Phys. Chem. A* **2011**, *115*, 392−401.
(21) Miertus, S.; Scrocco, E.; Tomasi, J. *Chem. Phys.* **1981**, *55*, 117−129.
(22) Tomasi, J.; Mennucci, B.; Cammi, R. *Chem. Rev.* **2005**, *105*, 2999−3093.
(23) Christiansen, O.; Mikkelsen, K. V. *J. Chem. Phys.* **1999**, *110*, 1365−1375.
(24) Christiansen, O.; Mikkelsen, K. V. *J. Chem. Phys.* **1999**, *110*, 8348−8360.
(25) Cammi, R. *J. Chem. Phys.* **2009**, *131*, 164104.
(26) Olivares del Valle, F.; Tomasi, J. *Chem. Phys.* **1991**, *150*, 139−150.
(27) Aguilar, M.; Olivares del Valle, F.; Tomasi, J. *Chem. Phys.* **1991**, *150*, 151−161.
(28) Caricato, M.; Scalmani, G.; Trucks, G. W.; Frisch, M. J. *J. Phys. Chem. Lett.* **2010**, *1*, 2369−2373.
(29) Purvis, G. D.; Bartlett, R. J. *J. Chem. Phys.* **1982**, *76*, 1910−1918.
(30) Salter, E. A.; Trucks, G. W.; Bartlett, R. J. *J. Chem. Phys.* **1989**, *90*, 1752−1766.
(31) Gauss, J.; Stanton, J. F.; Bartlett, R. J. *J. Chem. Phys.* **1991**, *95*, 2623−2638.
(32) Caricato, M. *J. Chem. Phys.* **2011**, *135*, 074113.
(33) Caricato, M.; Scalmani, G.; Frisch, M. J. *J. Chem. Phys.* **2011**, *134*, 244113.
(34) Cammi, R.; Corni, S.; Mennucci, B.; Tomasi, J. *J. Chem. Phys.* **2005**, *122*, 104513.
(35) Corni, S.; Cammi, R.; Mennucci, B.; Tomasi, J. *J. Chem. Phys.* **2005**, *123*, 134512.
(36) Caricato, M.; Mennucci, B.; Tomasi, J.; Ingrosso, F.; Cammi, R.; Corni, S.; Scalmani, G. *J. Chem. Phys.* **2006**, *124*, 124520.
(37) Osted, A.; Kongsted, J.; Mikkelsen, K. V.; Christiansen, O. *Mol. Phys.* **2003**, *101*, 2055−2071.
(38) Kongsted, J.; Pedersen, T. B.; Osted, A.; Hansen, A. E.; Mikkelsen, K. V.; Christiansen, O. *J. Phys. Chem. A* **2004**, *108*, 3632−3641.
(39) Cammi, R. *Int. J. Quantum Chem.* **2010**, *110*, 3040−3052.
(40) Cammi, R.; Fukuda, R.; Ehara, M.; Nakatsuji, H. *J. Chem. Phys.* **2010**, *133*, 024104.
(41) Fukuda, R.; Ehara, M.; Nakatsuji, H.; Cammi, R. *J. Chem. Phys.* **2011**, *134*, 104109.
(42) Cances, E.; Mennucci, B.; Tomasi, J. *J. Chem. Phys.* **1997**, *107*, 3032−3041.
(43) Mennucci, B.; Cances, E.; Tomasi, J. *J. Phys. Chem. B* **1997**, *101*, 10506−10517.
(44) Klamt, A.; Schüürmann, G. *J. Chem. Soc., Perkin Trans. 2* **1993**, 799−805.
(45) Cossi, M.; Rega, N.; Scalmani, G.; Barone, V. *J. Comput. Chem.* **2003**, *24*, 669−681.
(46) Scalmani, G.; Frisch, M. J. *J. Chem. Phys.* **2010**, *132*, 114110.
(47) Lipparini, F.; Scalmani, G.; Mennucci, B.; Cancès, E.; Caricato, M.; Frisch, M. J. *J. Chem. Phys.* **2010**, *133*, 014106.
(48) Marenich, A. V.; Cramer, C. J.; Truhlar, D. G.; Guido, C. A.; Mennucci, B.; Scalmani, G.; Frisch, M. *J. Chem. Sci.* **2011**, *2*, 2143−2161.
(49) Davidson, E. R. *J. Comput. Phys.* **1975**, *17*, 87−94.
(50) Rettrup, S. *J. Comput. Phys.* **1982**, *45*, 100−107.
(51) Hirao, K.; Nakatsui, H. *J. Comput. Phys.* **1982**, *45*, 246−254.
(52) Caricato, M.; Trucks, G. W.; Frisch, M. J. *J. Chem. Theory Comput.* **2010**, *6*, 1966−1970.
(53) Frisch, M. J.; Trucks, G. W.; Schlegel, H. B.; Scuseria, G. E.; Robb, M. A.; Cheeseman, J. R.; Scalmani, G.; Barone, V.; Mennucci, B.; Petersson, G. A.; Nakatsuji, H.; Caricato, M.; Li, X.; Hratchian, H. P.; Izmaylov, A. F.; Bloino, J.; Zheng, G.; Sonnenberg, J. L.; Hada, M.; Ehara, M.; Toyota, K.; Fukuda, R.; Hasegawa, J.; Ishida, M.; Nakajima, T.; Honda, Y.; Kitao, O.; Nakai, H.; Vreven, T.; Montgomery, J. A., Jr.; Peralta, J. E.; Ogliaro, F.; Bearpark, M.; Heyd, J. J.; Brothers, E.; Kudin, K. N.; Staroverov, V. N.; Keith, T.; Kobayashi, R.; Normand, J.; Raghavachari, K.; Rendell, A.; Burant, J. C.; Iyengar, S. S.; Tomasi, J.; Cossi, M.; Rega, N.; Millam, J. M.; Klene, M.; Knox, J. E.; Cross, J. B.; Bakken, V.; Adamo, C.; Jaramillo, J.; Gomperts, R.; Stratmann, R. E.; Yazyev, O.; Austin, A. J.; Cammi, R.; Pomelli, C.; Ochterski, J. W.; Martin, R. L.; Morokuma, K.; Zakrzewski, V. G.; Voth, G. A.; Salvador, P.; Dannenberg, J. J.; Dapprich, S.; Parandekar, P. V.; Mayhall, N. J.; Daniels, A. D.; Farkas, O.; Foresman, J. B.; Ortiz, J. V.; Cioslowski, J.; Fox, D. J. *Gaussian Development Version*, revision H.09+; Gaussian, Inc.: Wallingford, CT, 2010.
(54) Ho, J.; Klamt, A.; Coote, M. L. *J. Phys. Chem. A* **2010**, *114*, 13442−13444.
(55) Buswell, A. M.; Dunlop, E. C.; Rodebush, W. H.; Swartz, J. B. *J. Am. Chem. Soc.* **1940**, *62*, 325−328.
(56) Walsh, A. D. *Trans. Faraday Soc.* **1945**, *41*, 498−505.
(57) Mackinney, G.; Temmer, O. *J. Am. Chem. Soc.* **1948**, *70*, 3586−3590.
(58) Forbes, W. F.; Shilton, R. *J. Am. Chem. Soc.* **1959**, *81*, 786−790.
(59) Inuzuka, K. *Bull. Chem. Soc. Jpn.* **1961**, *34*, 729−732.
(60) Becker, R. S.; Inuzuka, K.; King, J. *J. Chem. Phys.* **1970**, *52*, 5164−5170.
(61) Staley, S. W.; Norden, T. D. *J. Am. Chem. Soc.* **1984**, *106*, 3699−3700.
(62) Aquilante, F.; Barone, V.; Roos, B. O. *J. Chem. Phys.* **2003**, *119*, 12323−12334.

(63) Losa, A. M.; Galvan, I. F.; Aguilar, M. A.; Martin, M. E. *J. Phys. Chem. B* **2007**, *111*, 9864−9870.
(64) Aidas, K.; Møgelhøj, A.; Nilsson, E. J. K.; Johnson, M. S.; Mikkelsen, K. V.; Christiansen, O.; Söderhjelm, P.; Kongsted, J. *J. Phys. Chem. A* **2008**, *109*, 8001−8010.
(65) Caricato, M.; Mennucci, B.; Scalmani, G.; Trucks, G. W.; Frisch, M. J. *J. Chem. Phys.* **2010**, *132*, 084102.
(66) Dunning, T. H. *J. Chem. Phys.* **1989**, *90*, 1007−1023.
(67) Rappe, A. K.; Casewit, C. J.; Colwell, K. S.; Goddard, W. A.; Skiff, W. M. *J. Am. Chem. Soc.* **1992**, *114*, 10024−10035.